inorganics

MDPI

Article

Accessing Bisphosphine Copper(I) Complexes with Recalcitrant Pterin–Phenanthroline Ligands Through Mechanochemistry

Siva S. M. Bandaru *, Christian Fischer, Jevy V. Correia, Anna-Lena Land and Carola Schulzke *

Bioanorganische Chemie, Institut für Biochemie, Universität Greifswald, Felix-Hausdorff-Str. 4, 17489 Greifswald, Germany; jevy.correia@uni-greifswald.de (J.V.C.); anna-lena.land@uni-greifswald.de (A.-L.L.)

* Correspondence: siva.bandaru@uni-greifswald.de (S.S.M.B.); carola.schulzke@uni-greifswald.de (C.S.)

Abstract: The synthesis of [Cu(PteN^N)(P^P)][BF_4] complexes with pterin-fused phenanthroline (PteN^N) derivatives and bisphosphine (P^P) co-ligands was achieved through a mechanochemical approach. Due to the extremely poor solubility of PteN^N ligands, traditional solution methods are ineffective, whereas solid-state mechanochemistry reliably yielded the targeted heteroleptic—rather than homoleptic—complexes with considerable stability even in solution. The transformation from ligand to complex increased the solubility dramatically. The ligands and complexes were comprehensively characterised with a mixture of routine spectroscopic and spectrometric methods, the applicability of which depended to some extent on the compounds' solubility, e.g., in the case of NMR spectroscopy. The photophysical properties of the complexes, which were not as exciting as anticipated, were assessed by absorption and emission spectroscopic methods, showing that further improvements are needed in complex design if these species are to be developed towards photocatalysis in the future.

Keywords: mechanochemistry; copper complexes; pterin; phenanthroline; bisphosphine; heteroleptic complexes

check for updates

Academic Editors: Debbie C. Crans and David Morales-Morales

Received: 24 April 2025
Revised: 15 May 2025
Accepted: 20 May 2025
Published: 22 May 2025

Citation: Bandaru, S.S.M.; Fischer, C.; Correia, J.V.; Land, A.-L.; Schulzke, C. Accessing Bisphosphine Copper(I) Complexes with Recalcitrant Pterin–Phenanthroline Ligands Through Mechanochemistry. *Inorganics* **2025**, *13*, 175. https://doi.org/10.3390/inorganics13060175

Copyright: © 2025 by the authors. Licensee MDPI, Basel, Switzerland. This article is an open access article distributed under the terms and conditions of the Creative Commons Attribution (CC BY) license (https://creativecommons.org/licenses/by/4.0/).

1. Introduction

Using sunlight for visible-light-mediated photocatalysis in organic synthesis has become a critically important strategy [1–3]. Molecular photosensitizers such as ruthenium polypyridyl and iridium phenylpyridine complexes are extensively utilised in these processes [4–6]. In the search for efficient photosensitizers, the exploration of copper(I) complexes has shown considerable promise due to their cost-effectiveness and significant photophysical properties [7,8]. When they were initially studied, mononuclear Cu^+ complexes such as $[Cu(phen)_2]^+$ (where phen = 1,10-phenanthroline and its derivatives) were found to exhibit limited luminescence in solution, primarily due to excited-state flattening distortions [9]. Innovations by researchers such as McMillin and Sauvage introduced bulky substituents at the 2,9-positions of 1,10-phenanthroline or substituted one phenanthroline ligand with a chelating bisphosphine, the bite angle of which may be varied, that significantly enhanced the emission quantum yields and extended the excited-state lifetimes of these complexes [10–12].

Today, a variety of well-defined homoleptic [13,14] and heteroleptic bis-diimine copper(I) complexes [15,16], $[Cu(N^N)_2]^+$, along with the heteroleptic diimine–bisphosphine copper(I) complexes $[Cu(N^N)(P^P)]^+$ and $[Cu(N^N)(N^P)]^+$ have been studied (Figure 1). In order to improve the absorption profile in the visible light region, π-extended diimine ligands have also been used for heteroleptic complex formation (Figure 1) [17,18]. These

complexes offer appropriate redox potentials and display excited-state lifetimes suitable for photocatalytic applications. Despite the significant potential of the copper complexes referred to above, there is still room for further development so as to fully exploit the abilities of these non-noble metal systems as catalysts.

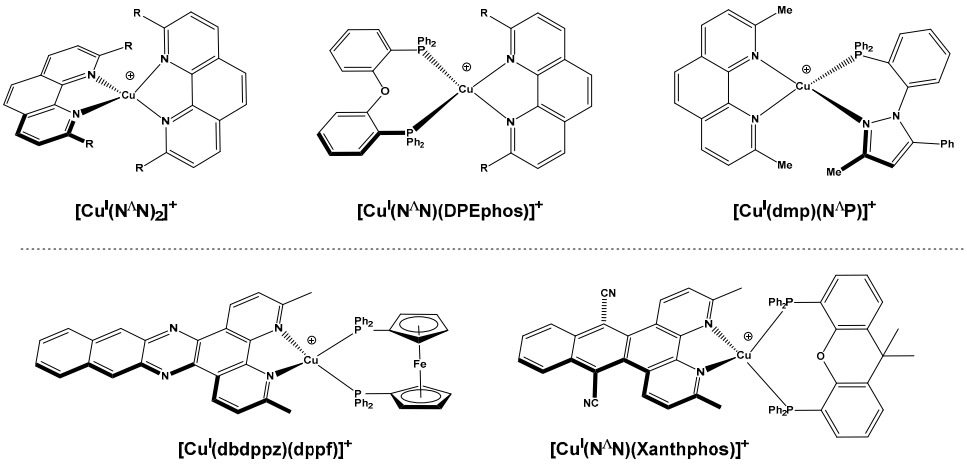


Figure 1. Selected examples of copper(I) photocatalysts.

Pterins are N-hetero-bi-cyclic molecules which exhibit quite unique electronic structures and chemical behaviour [19,20]. Derivatives thereof are found in nature as parts of biomolecules with a variety of important functions, and some have even been shown to be effective photosensitizers in the oxidation of, for instance, nucleic acids, which includes the unsubstituted parent structure [21–28]. Since, in our lab, pterin species are readily available for employment in a different project, we deemed it worth trying to combine the copper(I) photocatalysis field with pterin chemistry. This study, hence, demonstrates the synthesis and properties of a set of six pterin-fused phenanthroline–bisphosphine–copper(I) complexes, [Cu(PteN^N)(P^P)]$^+$, with some small variation in either of the two ligand types. Complexes with pterin structural motifs were previously shown to hold significant promise even in a biological context. Bis(bipyridyl) Ru^{2+} complexes with pteridinyl–phenanthrolines have effectively intercalated with DNA and RNA and acted as robust molecular "light switches" [29–32], and a tricarbonyl Re^+ complex with merely the unsubstituted pterin as a ligand was shown to photo-induce structural changes in DNA [33]. We therefore anticipated a significantly useful photochemical behaviour of the targeted and realized pterin-bearing copper(I) complexes with bisphosphine co-ligands.

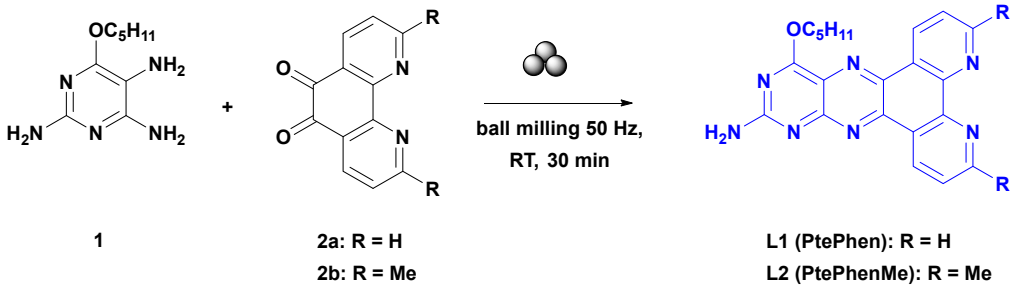
The typical synthesis of complexes relatively similar to our target species involves the use of dry dichloromethane, to which diimine ligands are added first, followed by diphosphine ligands an hour later, and stirring of the reaction mixture for extended periods ranging from 2 to 14 h [34–36]. While this method has proven effective for creating both homoleptic and heteroleptic copper(I) complexes with aromatic functionalized phenanthroline diamine ligands, it encounters challenges when extending the π-system or incorporating hydrogen-bonding prone backbones like a pterin [37] through fusion to the phenanthroline chelate. These modifications often lead to solubility issues in conventional organic solvents, potentially resulting in poor conversion rates or complex mixtures of homoleptic and heteroleptic compounds that are difficult to isolate and purify.

To address these issues, a mechanochemical solid-state reaction approach was chosen, which offers a sustainable alternative, particularly for substances with low solubility [38]. Mechanochemical synthesis comes with significant advantages, including eliminating the use of potentially toxic solvents and reducing the need for multiple purification and drying steps, thereby minimising waste generation [39]. The reactive extrusion process

was identified by IUPAC in 2019 as one of ten chemical innovations with the likeliest chance of impacting our world the most [40]. The benefits of mechanochemical methods are well known; yet, until now, they have very much been underexplored with regard to pterin chemistry, and they have never been applied in order to coordinate pterin-bearing ligands to copper centres. With regard to the six new complexes ([Cu(NˆN)(PˆP)][BF_4]) reported here, they have only become accessible by employing a ball milling method, while syntheses in solution have failed to give reasonable results. Comprehensive analyses including elemental analysis, ESI-MS, NMR, and UV/Vis spectroscopy measurements have been conducted on all complexes. In this report, we focus primarily on a very successful synthesis procedure for these complexes and their characterisation, as well as taking a tentative look at their photophysical properties, which, unfortunately, did not live up to the expectations that motivated this work in the first place.

2. Results and Discussion

Predominantly inspired by the work of James and co-workers toward the synthesis of salen ligands through ball milling [41], we adopted a relatively similar approach to synthesise our target ligands. Two pteridinyl–phenanthroline derivatives were successfully prepared: 13-(pentyloxy)pteridino [6,7-f][1,10]phenanthrolin-11-amine (**L1**; PtePhen) and its dimethyl derivative, 3,6-dimethyl-13-(pentyloxy)pteridino[6,7-f][1,10]phenanthrolin-11-amine (**L2**; PtePheMe). These were synthesised by reacting diamino pteridinyl derivative **1** with 5,6-dione phenanthroline **2** as solids using a standard ball milling vibrator set to a fixed frequency of 50 Hz (Scheme 1; Figure 2a). This mechanochemical method proved effective in providing these relatively complex chemical structures with high purity and in quantitative yields.



Scheme 1. Synthesis of pteridinyl-phenanthroline NˆN chelates via mechanochemical ball milling.

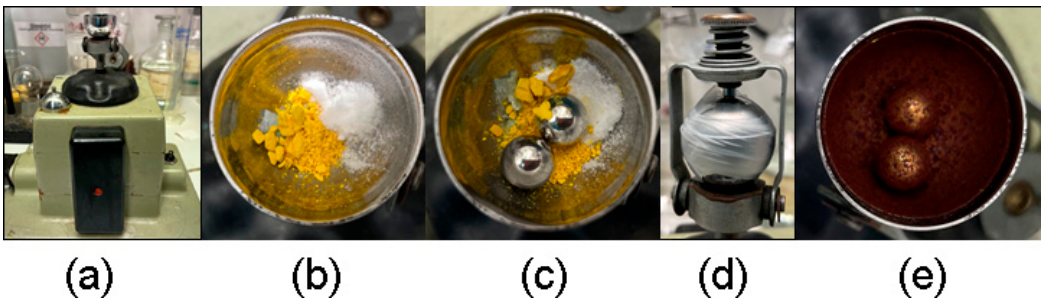
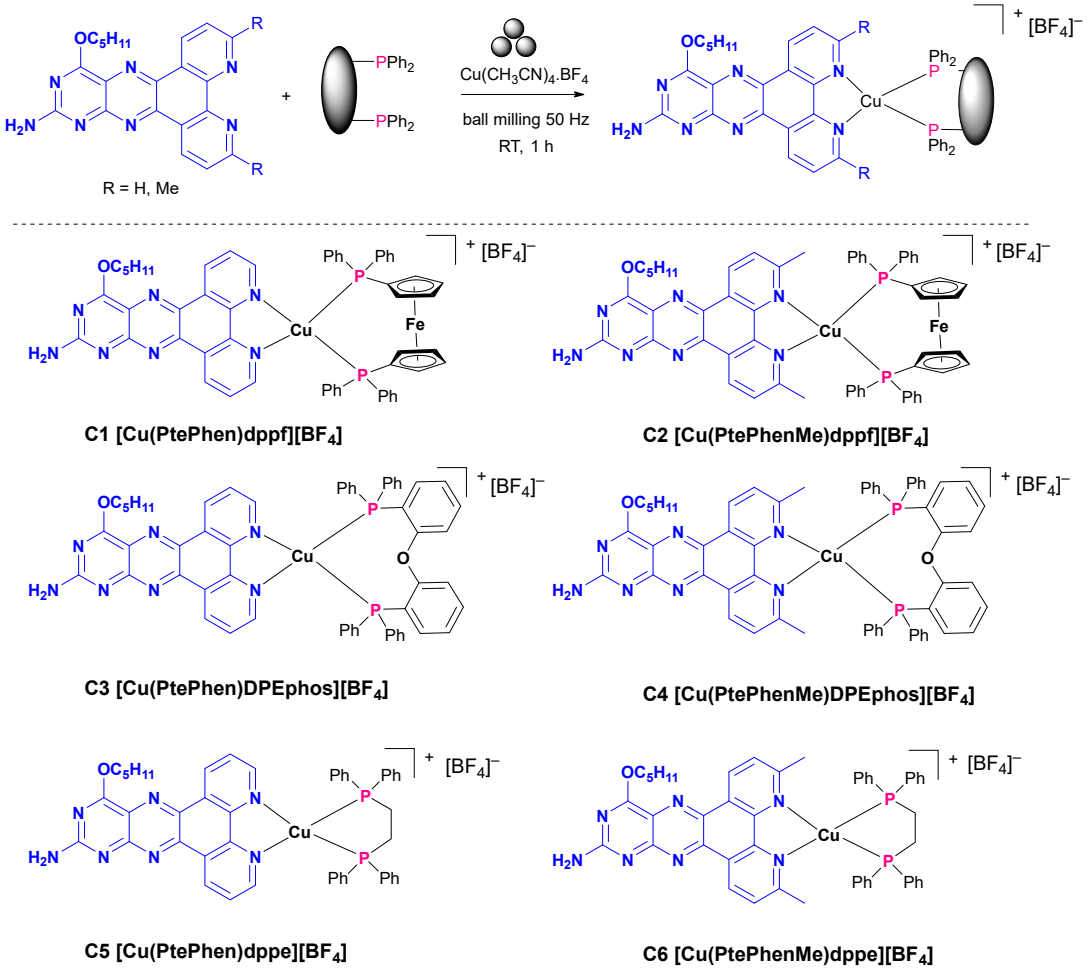


Figure 2. Mechanochemistry: (**a**) ball milling vibrator device; (**b**) starting materials added into milling jar; (**c**) addition of 6 mm stainless steel balls; (**d**) sealing jar and mounting on ball milling device; (**e**) product after completion of reaction.

In our initial attempts to synthesise the heteroleptic complexes, we employed equimolar ratios of Ligand **L1**, 1,1′-bis(diphenylphosphino)ferrocene (dppf), and [Cu(CH_3CN)$_4$][BF_4] in dry dichloromethane, allowing the reaction to proceed for 3–12 h at room temperature under a N_2 atmosphere. However, the ^{1}H and ^{31}P NMR analyses of the crude

reaction mixtures revealed predominantly unreacted starting materials with only trace amounts of the desired heteroleptic complex. Given the poor solubility of **L1** and **L2** in common solvents such as $CHCl_3$, CH_2Cl_2, and DMSO, and the inherent instability of the products in solution, a mechanochemical multi-component synthetic approach emerged as a superior alternative. Such an approach is anything but unheard of in copper complex chemistry [42–51], and in one study, rather similar complex salts to those in this work were prepared mechanochemically; this, most notably, was carried out using a mortar and pestle [52]. It should be noted, though, that while the application of mechanical force for the synthesis of copper complexes is relatively well known, the opposite is true for mechanochemical pterin synthesis [53]. Such a solvent-free method obviously improves the environmental sustainability of the process. In addition, in the case of the heteroleptic species of the type studied here, the solid-state strategy even maintained the stability of the $[Cu(N^{\wedge}N)(P^{\wedge}P)]^+$ complexes, which are known to be more stable in their solid form, and thereby less prone to dynamic ligand exchange reactions, that may disrupt the desired heteroleptic/homoleptic ratio, which should be as high as possible. This approach mitigates the challenges faced in traditional synthesis in solution, and presents a substantially more effective route for obtaining these complexes [54].

A series of Cu(I) pteridinyl–phenanthroline bis(phosphine) complexes (**C1**–**C6**) was synthesised by adding Ligand **L1** or **L2**, bis(phosphine) chelates (dppf, DPEphos, dppe), and $[Cu(CH_3CN)_4][BF_4]$ in a 1:1:1 ratio into a ball milling jar (Scheme 2; Figure 2b). In this study, two 6 mm stainless steel balls were uniformly used for the milling process (Figure 2c). The reaction vessel, sealed with paraffin film, was mounted on an in-house-made ball milling vibrator set to 50 Hz (Figure 2a,d) and milled for one hour. This resulted in the formation of yellow-orange-to-red solid substances. Analytically pure complexes were isolated afterwards in good yields by precipitating them from a 5 mL CH_2Cl_2 solution using an excess of diethyl ether. The ^1H, ^{31}P NMR spectroscopic, and ESI-MS spectrometric analyses confirmed the presence of only the heteroleptic complexes in all ligand combinations with essentially full conversion. Since Garra et al., in their mortar-and-pestle study, used very similar ligands and a complex salt ($[Cu(PhenMe)DPEphos][BF_4]$ [52], which distinguishes itself from **C4** only by its lack of a pterin moiety, the specific mechanochemical synthetic methodologies and their efficacies are very well comparable. The major conformity between the two approaches is the absence of any additive solvent during the mechanochemical treatment. The differences comprise (i) the consecutive (Garra et al.) or simultaneous addition off the starting materials, (ii) the type of application of mechanical force (manual (Garra et al.) with a mortar and pestle or instrumental using a ball mill), and (iii) the duration of the mechanical force applied (5 min and 10 s by Garra et al. or 60 min). The ball milling would likely have been successful even under a much shorter application time. However, since the reaction took place inside a sealed vessel, it was impossible to visually assess its progression via the colour change from mixture to product in contrast to the mortar-and-pestle study. Therefore, a longer period was chosen to make sure that the transformation was successfully completed. That the concomitant coordination of the two different ligands was quite successful implies that it is indeed not even necessary to coordinate the bulkier ligand first before adding the less bulky one. We consider this to be an advantage over the previously published synthesis method. Unfortunately, Garra et al. did not add any purification steps to their procedure and only report an NMR-purity yield of $\geq$95%, whereas in our case, the bulk material was purified by dissolving and re-precipitating it, and the isolated yield after purification was 85%. Presumably, the effectiveness of both approaches is essentially the same with regard to the yield, which can be considered quantitative.



Scheme 2. Syntheses of heteroleptic [Cu(PtePhenN^N)(P^P)][BF4] complexes (**C1**–**C6**) by ball milling.

The observed broadening and downfield shifting of signals corresponding to the phenanthroline moieties in the ^{1}H NMR spectra of complexes **C1**–**C6** are consistent with copper(I) coordination and increased quadrupolar relaxation effects. Although full high-resolution spectra of the free ligands were not obtained due to solubility limitations (particularly for **L1**), a representative ^{1}H NMR spectrum of **L2** in MeOD is provided in the Supporting Information for reference (Figure S10). Additionally, broad ^{31}P NMR signals for these complexes range from −3 ppm to −14 ppm, likely due to the quadrupolar nature of the copper nucleus, as previously reported (Figure 3) [54]. Cu^{+} complexes, known for their kinetic lability, often undergo ligand exchange in solution, even at room temperature [55]. The stability of complex **C1** was further assessed by monitoring its ^{31}P NMR spectrum in the non-coordinating solvent dichloromethane-d_2. After 24 h at room temperature, the ^{31}P NMR spectrum showed signals at +28.2 ppm and −8.5 ppm, with the former likely indicating the formation of a homoleptic $[Cu(dppf)_2][BF_4]$ complex salt (Figure S1, ESI) [56].

The bite angle of the chelating bisphosphine significantly affects the homoleptic/heteroleptic ratio. Smaller bite angles, such as with dppe, allow the Cu^{+} centre to accommodate two ligands of this type, facilitating homoleptic complexes [57]. Conversely, wider P-Cu-P angles (113–118°) in ligands, such as with dppf and DPEphos, tend to destabilise homoleptic $[Cu(P^{\wedge}P)_2]^{+}$ complexes [58]. Temperature-dependent ^{31}P NMR studies of complexes **C5** and **C6** showed that [Cu(PtePhen)(dppe)][BF_4] (**C5**) exhibited no change in its ^{31}P NMR spectrum, even when measured at −60 °C to raise the visibility of minor species (Figure S2, ESI). However, [Cu(PtePhenMe)(dppe)][BF_4] (**C6**) displayed a signal at −7.4 ppm at room temperature and an additional new broad signal at +7.5 ppm at

−60 °C, in accordance with previously reported data [56] for $[Cu(dppe)_2][BF_4]$, which thereby confirms its presence in the solution (Figure S2, ESI).

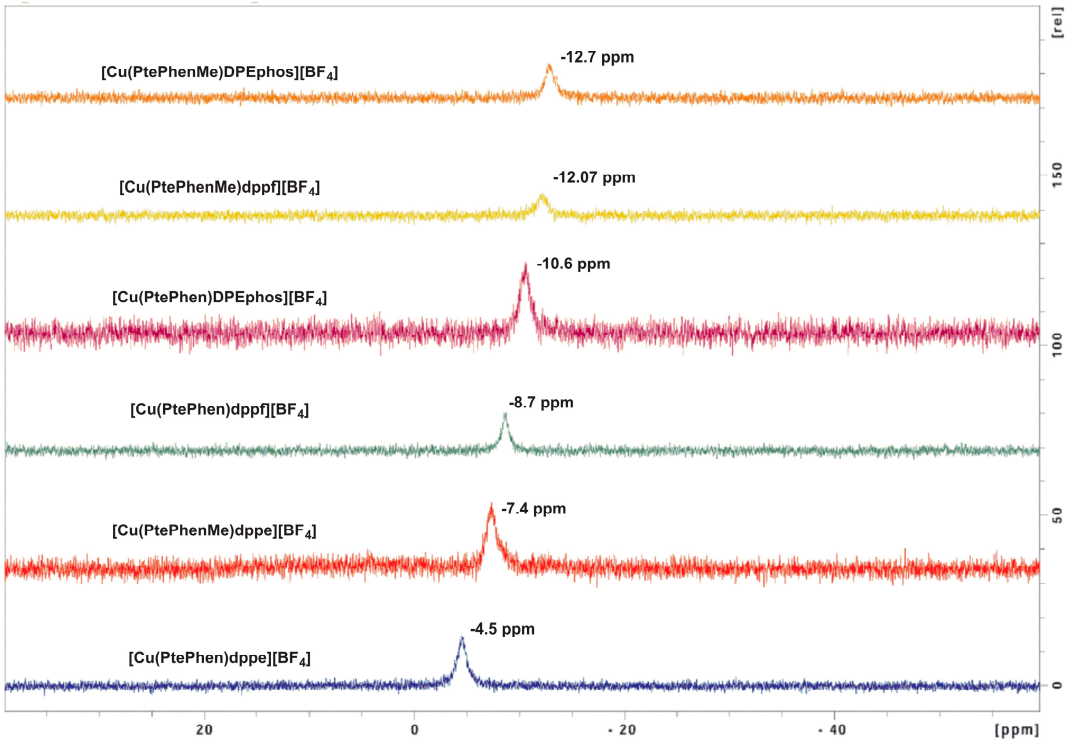


Figure 3. ^{31}P NMR spectra of complexes **C1–C6** in CD_2Cl_2 at room temperature.

ESI-MS mass spectrometry analysis of samples dissolved in methanol verified the presence of a single species for complexes **C1** through **C5**. However, for complex **C6**, the analysis revealed a mass peak at 860 m/z corresponding to the $[Cu(dppe)_2]^+$ homoleptic complex, alongside a molecular ion peak at 874 m/z for the heteroleptic complex $[Cu(PtePheMe)(dppe)][BF_4]$.

Complexes **C1–C6** exhibit bright yellow to orange and red colours. However, **C5** and **C6** were excluded from preliminary UV/Vis data evaluations and more detailed investigations due to the observed and/or likely thermodynamic equilibrium between heteroleptic and homoleptic complexes in solution (their spectra are shown in the ESI; Figures S4 and S5). Notably, complexes **C1–C4** demonstrate excellent solubility across a range of solvents, from protic to aprotic. This characteristic prompted us to explore the solvatochromic effects on their absorption maxima. Consequently, we recorded the electronic absorption spectra of complexes **C1–C4** in four different solvents with varied dielectric constants, spanning from polar protic (MeOH, dipole moment: 1.69 D) to merely polar (CH_2Cl_2, 1.62 D), and to more polar aprotic solvents (DMF, 3.82 D; DMSO, 3.96 D).

The UV-Vis absorption spectra of complexes **C1–C4** in various solvents exhibit a broad absorption band in the visible region attributed to metal-to-ligand charge transfer (MLCT) transitions, and ligand-centred absorption bands in the UV region (Table 1, spectra are provided in Figure 4a, and ESI, Figure S3) [59]. The MLCT bands of these complexes are notably intense, with absorption maxima ranging from 410 nm to 440 nm (Table 1). The molar extinction coefficients of **C1–C4** are nearly an order of magnitude higher than those of previously reported copper(I) diimine complexes, such as $[Cu(PheMe)_2]^+$ ($\varepsilon = 8 \times 10^3$ L·mol^{-1}·cm^{-1}) [60].

Table 1. The UV/Vis absorption and fluorescence emission profiles of complexes **C1–C4** in different solvent systems (DCM = dichloromethane; MeOH = methanol; DMF = dimethylformamide; DMSO = dimethylsulfoxide).

Comp.	DCM	MeOH	DMF	DMSO	Emission Profile (λ nm) [a]	
	λ_{max} nm [ε 10^4 $M^{-1}\cdot cm^{-1}$]				DMSO	MeOH
C1	410 (1.6) 320 (2.2) 285 (4.6)	425 (1.4) 320 (1.8) 290 (3.8)	430 (1.6) 330 (2.6) 300 (5.0)	440 (1.8) 330 (2.6) 290 (5.0)	497	504
C2	410 (1.6) 320 (1.4) 290 (4.6)	430 (1.4) 320 (2.0) 300 (4.0)	430 (1.4) 300 (4.6)	450 (1.6) 310 (4.8)	512	497
C3	410 (1.8) 290 (5.1)	420 (2.0) 280 (5.8)	420 (1.4) 290 (4.6)	440 (1.6) 290 (4.6)	502	494
C4	410 (1.6) 300 (5.0)	420 (1.6) 300 (4.6)	440 (1.6) 300 (4.8)	440 (1.6) 300 (4.0)	504	502

[a] A 1mM concentration was used for fluorescence emission measurements at an excitation wavelength of λ 400 nm.

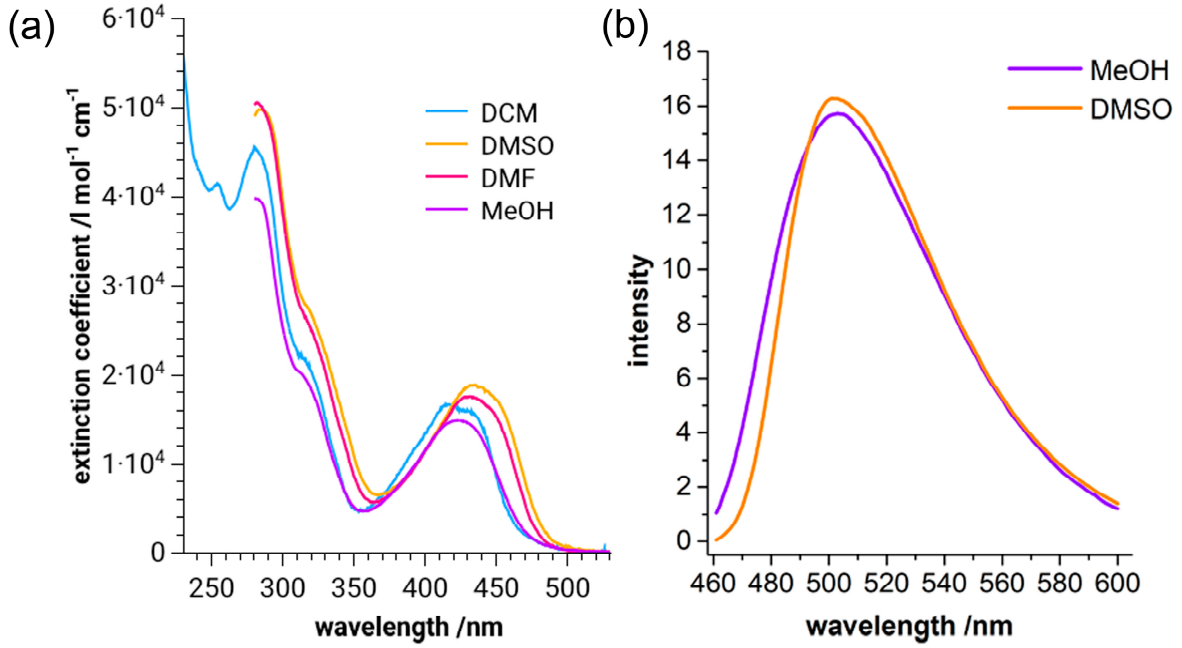


Figure 4. (**a**) UV-Vis absorption spectra for complex **C1**; (**b**) fluorescence emission spectra for complex **C1**. DCM = dichloromethane; DMSO = dimethylsulfoxide; DMF = dimethylformamide; MeOH = methanol.

Moreover, the high molar extinction coefficient values of the visible band (~2×10^4 $L\cdot mol^{-1}\cdot cm^{-1}$) signify a substantial enhancement in the light-absorbing properties of [Cu Pte(N^N)(P^P)][BF_4] complexes. Interestingly, a bathochromic shift of approximately 20–25 nm is observed when transitioning from methanol to more polar solvents. This shift may be attributed to interactions with the second coordination sphere, potentially affecting the geometry at the copper centre (more square-planar vs. more tetrahedral) and indicating solvent stabilisation of the excited state.

The Stokes shifts in the emission spectra of **C1–C4** range from 57 nm to 72 nm, indicating different levels of excited-state structural relaxation (Figure 4b; Figure S6 in the ESI). The comparatively low Stokes shift (~57 nm) of complex **C1** indicates little excited-state rearrangement. Although solvent interaction is limited by the structural stiffness of the

ligand framework, the slight redshift in the emission in MeOH suggests that the solvent polarity influences the excited state. Similar absorption characteristics are shared by **C1** and **C3** (440 nm in DMSO and 425–420 nm in MeOH); however, **C3** exhibits a slightly redshifted emission (502 nm in DMSO), suggesting a minor variation in excited-state dynamics. The least solvent-dependent behaviour is shown by **C4**, which has emissions at 504 nm (DMSO) and 502 nm (MeOH) and absorptions at 440 nm (DMSO) and 420 nm (MeOH). This implies a rigid ligand environment, which could lead to extended excited-state lifetimes. **C2** exhibits the most noticeable visible-light absorption and excited-state stabilisation, rendering it the most appropriate for potential future photoredox catalysis and investigations of energy transfer mechanisms. The excited-state energy levels (~2.42–2.49 eV) point to all four complexes as relatively promising candidates for photocatalytic applications. However, the quantum yields of the photo-excitations and relaxations, considering the available respective literature discussing related species [61–63], are not expected to be as high as was anticipated when designing the pterin-bearing ligand systems, and the energy profiles are also not as exceptional as initially envisioned. While **C1**'s comparatively high excited-state energy makes it more appropriate for reactions requiring high-energy charge transfer, the more moderate excited-state energy of **C3** and **C4** suggests that they may be better in facilitating both oxidative and reductive photocatalysis.

In future studies, we will further investigate these complexes by determining their quantum yields and excited-state lifetimes using time-resolved spectroscopy. Additionally, their photocatalytic performance may be tested in model reactions such as α-arylation and atom-transfer radical addition (ATRA). Finally, synthetic changes shall be made to the ligand systems employed to more comprehensively unlock the potential of the embedded pterin moieties. This will be facilitated by the observations of this study with regard to the mechanochemical ligand preparations.

3. Materials and Methods

All reactions were performed under ambient conditions in a stainless-steel jar on a ball mill vibrator (n.M:v. Ardenne, DDR-GM 9458, 220/110 V 30 W 50 Hz). The ^{1}H NMR (300 MHz), ^{13}C NMR (75 MHz), ^{31}P NMR (121 MHz), ^{11}B NMR (96 MHz), and ^{19}F NMR (282 MHz) spectra were recorded on a Bruker NMR Avance II 300 spectrometer, and the solvent residual peak (CD_2Cl_2 ^{1}H, δ = 5.32; ^{13}C, δ = 53.8) was used as an internal standard. Chemical shifts in the ^{1}H NMR spectra were recorded in delta (δ) units, in parts per million (ppm), relative to chemical shifts in TMS, and in deuterated solvent for the ^{13}C signals (CD_2Cl_2 δ 53.8 ppm), and ^{31}P NMR, ^{11}B NMR, and the ^{19}F NMR spectra were referenced according to the "unified scale" of IUPAC [64]. The peak multiplicities are specified as follows: s, singlet; d, doublet; t, triplet; q, quartet; m, multiplet; br, broad. The ESI-MS (m/z) spectra were obtained on an ADVION Express mass spectrometer with methanol as an injection solvent. The UV-Vis spectra were recorded on a Perkin Elmer Lambda 800 UV-Vis spectrophotometer. The fluorescence spectra were measured using a JASCO FP-6500 150W Xenon lamp and infrared spectra on an FT-IR spectrometer (Shimadzu IR-Affinity; range 7800–350 cm^{-1}). An Elementar vario MICRO cube was used to determine the elemental configurations of the final pure products experimentally. The starting material compounds, 1, 2 and $[Cu(CH_3CN)_4][BF_4]$, were synthesised and purified according to the literature reports [65–67].

3.1. Synthesis of N^N Chelate Ligands PtePhen (L1) and PtePhenMe (L2) by Mechanochemical Solid-State Ball Milling

General Procedure (GP1): Equimolar amounts of 6-(pentyloxy)pyrimidine-2,4,5-triamine (1) and either 1,10-phenanthroline-5,6-dione (2a) or 2,9-dimethyl-1,10-phenanthroline-5,6-

dione (2b) were added to a clean, dry stainless-steel jar under ambient conditions. To this, two 6 mm stainless steel balls were introduced. The mixture was then subjected to ball milling on a vibrator set to a frequency of 50 Hz. The progress of the reaction was monitored using thin-layer chromatography (TLC) with a chloroform/methanol (9:1) mobile phase. The resulting bright yellow solid, which exhibited poor solubility in chloroform, dichloromethane (DCM), and diethyl ether, was washed with minimal amounts of cold DCM followed by an excess of diethyl ether. It was then dried under reduced pressure to yield analytically pure compounds L1 or L2 as bright yellow fluffy solids.

Ligand **L1**—PtePhen: 13-(pentyloxy)pteridino [6,7-f][1,10]phenanthrolin-11-amine: The general procedure (GP1) was followed by using 6-(pentyloxy)pyrimidine-2,4,5-triamine (211.3 mg, 1 mmol) and 1,10-phenanthroline-5,6-dione (210.2 mg, 1 mmol), yielding the desired 13-(pentyloxy)pteridino [6,7-f][1,10]phenanthrolin-11-amine (300 mg, 0.778 mmol, 78%) as a bright yellow fluffy solid. Due to the poor solubility in CD_2Cl_2, $CDCl_3$, DMSO (d_6), and CD_3COOD NMR solvents, high-resolution NMR was impossible to record. CHN: Calc. for $C_{21}H_{19}N_7O$: C, 65.44; H, 4.97; N, 25.44; Found: C, 64.62; H, 4.75; N, 25.49. APCI-MS: Calc. for $C_{21}H_{19}N_7O$: 385.431 m/z, found $[M+H]^+$: 386.7 m/z. IR (KBr, ν, selected peak, cm^{-1}): 3262, 3180, 3079, 2955, 2870, 1623, 1605, 1592, 1512, 1462, 1437, 1413, 1395, 1361, 1331, 1210, 1165, 1129, 1022, 819, 744.

Ligand **L2**—PtePhenMe: 3,6-dimethyl-13-(pentyloxy)pteridino [6,7-f][1,10]phenanthrolin-11-amine: The general procedure (GP1) was followed by using 6-(pentyloxy)pyrimidine-2,4,5-triamine (211.3 mg, 1 mmol) and 2,9-dimethyl-1,10-phenanthroline-5,6-dione (238.2 mg, 1 mmol), yielding the desired 13-(pentyloxy)pteridino [6,7-f][1,10]phenanthrolin-11-amine (326 mg, 0.79 mmol, 79%) as a bright orange-yellow fluffy solid. Due to the poor solubility in CD_2Cl_2, $CDCl_3$, DMSO (d_6), and CD_3COOD NMR solvents, high-resolution NMR was impossible to record. A reasonably resolved ^{1}H-NMR spectrum is provided in the ESI in Figure S10. ^{1}H NMR (300 MHz, CD_3OD) δ ppm: 9.33–9.39 (dd, 1 H), 9.23 (d, J = 8.34 Hz, 1 H), 7.67–7.77 (m, 2 H), 4.61–4.73 (t, J = 6.97 Hz, 2 H), 2.92 (s, 3 H), 2.90 (s, 3H), 1.96–2.08 (m, 2 H), 1.45–1.66 (m, 4 H), 0.97–1.09 (m, 3 H).CHN: Calc. for $C_{23}H_{23}N_7O$: C, 66.81; H, 5.61; N, 23.71; Found: C, 65.14; H, 5.45; N, 23.10. APCI-MS: Calc. for $C_{23}H_{23}N_7O$: 413.5 m/z, found $[M+H]^+$: 414.8 m/z. IR (KBr, ν, selected peak, cm^{-1}): 3315, 3214, 2956, 2858, 1595,1588, 1513, 1439, 1375, 1328, 1260, 1211, 1169, 1135, 1086, 1029, 973, 836, 751.

3.2. Synthesis of [Cu(PtePhenR N∧N) (PP)][BF_4] Complexes by Mechanochemical Soid-State Ball Milling

General procedure (GP2): Equimolar amounts of PtePhen N^N ligands, selected P^P ligands, and the $[Cu(CH_3CN)_4][BF_4]$ precursor were placed in a clean, dry stainless-steel jar. Two 6 mm stainless steel balls were added, and the assembly was attached to a vibrator device set to a frequency of 50 Hz. The mixture underwent solid-state ball milling for 1 h. N.B.: According to a preliminary monitored ^{31}P-NMR study with regard to the actual time needed for transformation, 30 min (possibly even less) is likely fully sufficient to facilitate the reaction. After milling, the resulting coloured solids were dissolved in 5 mL of dichloromethane (DCM) and then precipitated by adding an excess of diethyl ether with continuous stirring. The coloured precipitates were centrifuged, and the solids collected and dried under reduced pressure to yield analytically pure copper(I) complexes.

Synthesis of [Cu(PtePhen)dppf][BF_4] (**C1**): The general procedure GP2 was followed by using ligand L1 (30.8 mg, 0.08 mmol), dppf (46.6 mg, 0.08 mmol), and $[Cu(CH_3CN)_4][BF_4]$ (25 mg, 0.08 mmol), yielding the desired complex C2 as a yellow solid (76.7 mg, 0.076 mmol, 96%). ^{1}H NMR (300 MHz, CD_2Cl_2-d_2) δ ppm: 9.72 (d, J = 8.34 Hz, 1 H), 9.59 (d, J = 8.16 Hz, 1 H), 8.81 (d, J = 4.95 Hz, 1 H), 8.75 (d, J = 4.95 Hz, 1 H), 7.78–7.86 (m, 2 H), 7.31–7.40 (m, 4 H), 7.18–7.29 (m, 16 H), 5.87 (br. s., 2 H), 4.71 (t, J = 6.83 Hz, 2 H), 4.57 (s, 4 H), 4.41 (s, 4 H), 1.49–1.60 (m, 6 H), 0.92–1.09 (m, 3 H); ^{13}C NMR (75 MHz, CD_2Cl_2-d_2) δ ppm: 163,

155, 144.6, 133.3, 130.6, 129.1, 126.2, 74.9, 73.3, 69.5, 28.4, 22.7, 14.1; ^{31}P NMR (121 MHz, CD_2Cl_2-d_2) δ ppm: −8.5; ^{19}F NMR (282 MHz, CD_2Cl_2-d_2) δ ppm: −153.3, −153.4; ^{11}B NMR (96 MHz, CD_2Cl_2-d_2) δ ppm: −1.1; IR (KBr, ν, selected peak, cm^{-1}): 3378, 2955, 2857, 1611, 1598, 1513, 1465, 1435, 1395, 1361, 1328, 1165, 1084,1033, 820, 738,697; ESI-MS (m/z): Calcd for $[Cu(PtePhen)(dppf)]^+$: 1003.3 m/z, found: $[M+H]^+$ = 1004.2 m/z; CHN: Calc. for $C_{55}H_{47}BCuF_4FeN_7OP_2$: C, 65.84; H, 4.72; N, 9.77; Found: C, 65.57; H, 4.74; N, 9.73.

Synthesis of $[Cu(PtePhenMe)dppf][BF_4]$ (**C2**): The general procedure GP2 was followed by using ligand L2 (33.1 mg, 0.08 mmol), dppf (46.6 mg, 0.08 mmol), and $[Cu(CH_3CN)_4][BF_4]$ (25 mg, 0.08 mmol), yielding the desired complex C2 as an orange-yellow solid (67.4 mg, 0.069 mmol, 87%). ^{1}H NMR (300 MHz, CD_2Cl_2-d_2) δ ppm: 9.70 (d, J = 8.34 Hz, 1 H), 9.58 (d, *J* = 8.44 Hz, 1 H), 7.66 (d, *J* = 7.89 Hz, 2 H), 7.31 (d, *J* = 6.42 Hz, 4 H), 7.11–7.25 (m, 16 H), 5.83 (br. s., 2 H), 4.80 (d, *J* = 1.74 Hz, 4 H), 4.69 (s, 4 H), 2.35 (d, *J* = 3.39 Hz, 6 H), 1.54–1.61 (m, 6 H), 0.97–1.05 (m, 3 H); ^{13}C NMR (75 MHz, CD_2Cl_2-d_2) δ ppm: 160.9, 156.8, 143.4, 134.2, 132.5, 130.4, 129.0, 75.2, 73.2, 69.5, 28.5, 22.8, 18.9, 14.1; ^{31}P NMR (121 MHz, CD_2Cl_2-d_2) δ ppm: −12.3; ^{19}F NMR (282 MHz, CD_2Cl_2-d_2) δ ppm: −153.3, −153.4; ^{11}B NMR (96 MHz, CD_2Cl_2-d_2) δ ppm: −1.11; IR (KBr, ν, selected peak, cm^{-1}): 3360, 3057, 2954, 2869, 1619, 1599, 1509, 1449, 1435, 1327, 1165, 1084, 1033, 972, 840, 745, 698; ESI-MS (m/z): Calcd for $[Cu(PtePhenMe)(dppf)]^+$: 1031.4 m/z, found: $[M+H]^+$: 1032.6 m/z; CHN: Calc. for $C_{57}H_{51}BCuF_4FeN_7OP_2$: C, 66.38; H, 4.98; N, 9.51; Found: C, 66.64; H, 4.67; N, 9.77.

Synthesis of $[Cu(PtePhen)DPEphos][BF_4]$ (**C3**): The general procedure GP2 was followed by using ligand L1 (30.8 mg, 0.08 mmol), DPEphos (43.1 mg, 0.08 mmol), and $[Cu(CH_3CN)_4][BF_4]$ (25 mg, 0.08 mmol), yielding the desired complex C3 as a yellow solid (73.4 mg, 0.074 mmol, 93%). ^{1}H NMR (300 MHz, CD_2Cl_2-d_2) δ ppm: 9.65 (d, J = 8.07 Hz, 1 H), 9.51 (d, *J* = 7.98 Hz, 1 H), 8.76 (d, *J* = 4.68 Hz, 1 H), 8.80 (d, *J* = 4.86 Hz, 1 H), 7.72–7.83 (m, 2 H), 7.31–7.40 (m, 2 H), 7.21–7.31 (m, 4 H), 7.09–7.20 (m, 10 H), 6.96–7.09 (m, 10 H), 6.74–6.91 (m, 2 H), 5.91 (br. s., 2 H), 4.71 (t, *J* = 6.79 Hz, 2 H), 1.43–1.66 (m, 6 H), 0.94–1.07 (m, 3 H); ^{13}C NMR (75 MHz, CD_2Cl_2-d_2) δ ppm: 158.7, 150.5, 140.8, 134.6, 133.3, 132.5, 130.9, 130.4, 129, 126.4, 125.5, 120.8, 69.5, 28.4, 22.7, 20.8, 14.1; ^{31}P NMR (121 MHz, CD_2Cl_2-d_2) δ ppm: −10.6; ^{19}F NMR (282 MHz, CD_2Cl_2-d_2) δ ppm: −153.3, −153.4; ^{11}B NMR (96 MHz, CD_2Cl_2-d_2) δ ppm: −1.1; IR (KBr, ν, selected peak, cm^{-1}): 3376, 3063, 2955, 2867, 1598, 1513, 1463, 1436, 1396, 1361, 1328, 1259, 1222, 1167, 1124, 1084, 875, 820, 745, 698; ESI-MS (m/z): Calcd for $[Cu(PtePhenM)(DPEphos)]^+$: 987.2 m/z, found: $[M+H]^+$: 988.3 m/z; CHN: Calc. for $C_{52}H_{36}BCuF_4N_7OP_2$: C, 63.27; H, 3.68; N, 9.93; Found: C, 62.48; H, 4.02; N, 9.03.

Synthesis of $[Cu(PtePhenMe)DPEphos][BF_4]$ (**C4**): The general procedure GP2 was followed by using ligand L2 (33.1 mg, 0.08 mmol), DPEphos (43.1 mg, 0.08 mmol), and $[Cu(CH_3CN)_4][BF_4]$ (25 mg, 0.08 mmol), yielding the desired complex C4 as an orange-yellow solid (69 mg, 0.068 mmol, 85%). ^{1}H NMR (300 MHz, CD_2Cl_2-d_2) δ ppm: 9.49–9.62 (m, 1 H), 9.45 (d, *J* = 8.34 Hz, 1 H), 7.70 (d, *J* = 8.34 Hz, 2 H), 7.34–7.42 (m, 2 H), 7.26 (d, *J* = 8.07 Hz, 3 H), 7.22 (br. s., 5 H), 6.97–7.09 (m, 18 H), 5.87 (br. s., 2 H), 4.70 (t, *J* = 6.83 Hz, 2 H), 2.48 (s, 6 H), 1.50–1.64 (m, 6 H), 0.91–1.08 (m, 3 H); ^{13}C NMR (75 MHz, CD_2Cl_2-d_2) δ ppm: 158.7, 146.3, 134.1, 133.2, 133.1, 132.7, 132.2, 132, 130.2, 129, 128.9, 128.8, 126.9, 125.6, 120.5, 54.5, 54.1, 53.7, 53.4, 53, 28.4, 27.4, 22.7, 14.1; ^{31}P NMR (121 MHz, CD_2Cl_2-d_2) δ ppm: −12.7; ^{19}F NMR (282 MHz, CD_2Cl_2-d_2) δ ppm: −153.3, −153.4; ^{11}B NMR (96 MHz, CD_2Cl_2-d_2) δ ppm: −1.1; IR (KBr, ν, selected peak, cm^{-1}): 3352, 3054, 2955, 2859, 2387, 2307, 1619, 1599, 1577, 1509, 1460, 1436, 1327, 1260, 1220, 1170, 1124, 1084, 1063, 746, 697; ESI-MS (m/z): Calcd for $[Cu(PtePhenMe)DPEphos]^+$: 1015.3 m/z, found: $[M+H]^+$: 1016.9 m/z; CHN: Calc. for $C_{54}H_{40}BCuF_4N_7OP_2$: C, 63.88; H, 3.97; N, 9.66; Found: C, 62.91; H, 3.04; N, 8.98.

Synthesis of [Cu(PtePhen)dppe][BF_4] (**C5**): The general procedure GP2 was followed by using ligand L1 (38.5 mg, 0.1 mmol), dppe (39.8 mg, 0.1 mmol), and [Cu(CH_3CN)$_4$][BF_4] (31.5 mg, 0.1 mmol), yielding the desired complex C5 as an orange-red solid (74.5 mg, 0.088 mmol, 88%). ^{1}H NMR (300 MHz, CD_2Cl_2-d_2) δ ppm: 9.81 (d, *J* = 7.79 Hz, 1 H), 9.67 (d, *J* = 8.25 Hz, 1 H), 8.70–8.87 (m, 2 H), 7.99 (br. s., 2 H), 7.40 (br. s., 19 H), 7.20 (br. s., 1 H), 5.87 (br. s., 2 H), 4.71 (t, *J* = 6.51 Hz, 2 H), 2.76 (t, *J* = 5.32 Hz, 4 H), 1.50–1.64 (m, 6 H), 1.00 (t, *J* = 6.88 Hz, 3 H); ^{13}C NMR (75 MHz, CD_2Cl_2-d_2) δ ppm: 168.3, 163.1, 156.6, 152.5, 151.1, 146.8, 144.9, 141.6, 136.3, 134.7, 132.6, 132.5, 132.4, 132.2, 132, 131, 130.8, 129.7, 129.6, 129.6, 129.4, 126.5, 69.5, 54.5, 54.1, 53.7, 53.4, 53, 28.5, 28.4, 25.9 25.6, 22.8, 14.1; ^{31}P NMR (121 MHz, CD_2Cl_2-d_2) δ ppm: −4.5; ^{19}F NMR (282 MHz, CD_2Cl_2-d_2) δ ppm: −153.3, −153.4; ^{11}B NMR (96 MHz, CD_2Cl_2-d_2) δ ppm: −1.1; IR (KBr, ν, selected peak, cm^{-1}): 3352, 3054, 2955, 2930, 2869, 2359, 1653, 1617, 1576, 1525, 1448, 1436, 1399, 1361, 1327, 1292, 1268, 1213, 1171, 1057, 766, 745, 696, 515, 495; ESI-MS (*m*/*z*): Calcd for [Cu(PtePhen)dppe]$^+$: 847.1 *m*/*z*, found: [M+H]$^+$: 848.2 *m*/*z*; CHN: Calc. for $C_{42}H_{32}BCuF_4N_7P_2$: C, 59.55; H, 3.81; N, 11.58; Found: C, 58.74; H, 4.12; N, 10.78.

Synthesis of [Cu(PtePhenMe)dppe][BF_4] (**C6**): The general procedure GP2 was followed by using ligand L2 (41.4 mg, 0.1 mmol), dppe (39.8 mg, 0.1 mmol), and [Cu(CH_3CN)$_4$][BF_4] (31.5 mg, 0.1 mmol), resulting in the desired complex C6 as part of a mixture constituting a bright red solid after the purification attempt (68.2 mg, 0.078 mmol, 78%) (it had a 70:30 NMR-ratio of homoleptic to heteroleptic compounds). ^{1}H NMR (300 MHz, CD_2Cl_2-d_2) δ ppm: 9.72 (br. s., 1 H), 9.59 (t, *J* = 7.89 Hz, 1 H), 7.92 (d, *J* = 8.44 Hz, 1 H), 7.78 (d, *J* = 8.16 Hz, 1 H), 7.23–7.42 (m, 16 H), 7.14–7.23 (m, 12 H), 5.93 (br. s., 2 H), 4.72 (t, *J* = 6.51 Hz, 2 H), 3.04 (t, *J* = 5.82 Hz, 2 H), 2.52 (d, *J* = 3.94 Hz, 3 H), 2.43 (br. m., 3 H), 2.04–2.11 (m, 4 H), 1.96 (s, 2 H), 1.51–1.66 (m, 6 H), 1.00 (t, *J* = 7.01 Hz, 3 H); ^{13}C NMR (75 MHz, CD_2Cl_2-d_2) δ ppm: 162.3, 157.2, 144.9, 141.5, 134, 133.8, 132.5, 131.9, 131.8, 131.7, 130.8, 130.7, 129.6, 129.6, 129.5, 129.4, 126.8, 126.6, 66, 54.5, 54.3, 54.1, 54, 53.7, 53.6, 53.4, 53, 28.5, 28.4, 27.7. 27.5, 22.7, 15.4, 14.1; ^{31}P NMR (121 MHz, CD_2Cl_2-d_2) δ ppm: −7.4; ^{19}F NMR (282 MHz, CD_2Cl_2-d_2) δ ppm: −153.3, −153.4; ^{11}B NMR (96 MHz, CD_2Cl_2-d_2) δ ppm: −1.1; IR (KBr, ν, selected peak, cm^{-1}): 3350, 3056, 2933, 2869, 2348, 2333, 1699, 1686, 1653, 1617, 1576, 1523, 1448, 1436, 1399, 1361, 1327, 1292, 1268, 1222, 1213, 1171, 1057, 998, 870, 820, 766, 745, 696, 515, 495; ESI-MS (*m*/*z*): Calcd for[Cu(PtePhenMe)dppe]+: 875.1 *m*/*z*, [Cu(dppe)$_2$]+: 860.4 *m*/*z*, found: Heteroleptic [M+H]$^+$: 876 3 *m*/*z*, Homoleptic [M+H]$^+$: 861.2 *m*/*z*; CHN: Calc. for [$C_{44}H_{36}BCuF_4N_7P_2$ + 0.5 ($C_{52}H_{48}BCuF_4P_4$) + 4 (CH_3CN)]: C, 58.99; H, 4.57; N, 9.70. Found: C, 58.56; H, 4.67; N, 9.71.

4. Conclusions

In conclusion, we successfully synthesised [Cu^I(PteN^N)(P^P)][BF_4] complexes **C1–C6** using a mechanochemical ball milling process, which resulted in the first copper complexes bearing pterin-fused phenanthrolines as coordinated ligands. The green solid-state approach not only facilitated the generation of complexes **C1–C6**, but also proved critically important for the effective synthesis of the pterin–phenanthroline ligands in the first place considering their poor solubility in traditional organic solvents. Comprehensive characterisation of two ligands and six complexes was achieved through NMR (except for one ligand), FT-IR, ESI-MS, and CHN elemental analyses. Preliminary UV/Vis and fluorescence emission investigations of four complexes demonstrated moderately promising photocatalytic potential, with absorption maxima in the visible region (410–440 nm) exhibiting solvent-dependent shifts and an encouraging Stokes shift of up to 72 nm. Future work will focus on exploring the quantum yields and conducting detailed electrochemical studies to further evaluate the capabilities of this sub-family of copper(I) complexes in a photocatalytic context.

Supplementary Materials: The following supporting information can be downloaded at: https://www.mdpi.com/article/10.3390/inorganics13060175/s1: Figure S1: Stability study of complex **C1** in DCM for 24 h. Figure S2: ^{31}P NMR spectra for **C5** and **C6** at room temperature and −60 °C. Figure S3: UV-Vis absorption spectra for complexes **C1**–**C4**. Figure S4: UV-Vis spectra of **C5**. Figure S5: UV-Vis spectra of **C6**. Figure S6: Fluorescence emission spectra of complexes **C1**–**C4**. Figure S7: FT-IR spectrum of ligand L1. Figure S8: APCI-MS spectrum of ligand **L1**. Figure S9: FT-IR spectrum of ligand **L2**. Figure S10: ^{1}H NMR spectrum of ligand **L2** in MeOD. Figure S11: APCI-MS spectrum of ligand **L1**. Figure S12: ^{1}H NMR spectrum of complex **C1** in CD_2Cl_2. Figure S13: ^{13}C NMR spectrum of complex **C1** in CD_2Cl_2. Figure S14: ^{31}P NMR spectrum of complex **C1** in CD_2Cl_2. Figure S15: ^{1}H NMR spectrum of complex **C2** in CD_2Cl_2. Figure S16: ^{13}C NMR spectrum of complex **C2** in CD_2Cl_2. Figure S17: ^{31}P NMR spectrum of complex **C2** in CD_2Cl_2. Figure S18: ^{1}H NMR spectrum of complex **C3** in CD_2Cl_2. Figure S19: ^{13}C NMR spectrum of complex **C3** in CD_2Cl_2. Figure S20: ^{31}P NMR spectrum of complex **C3** in CD_2Cl_2. Figure S21: ^{1}H NMR spectrum of complex **C4** in CD_2Cl_2. Figure S22: ^{13}C NMR spectrum of complex **C4** in CD_2Cl_2. Figure S23: ^{31}P NMR spectrum of complex **C4** in CD_2Cl_2. Figure S24: ^{1}H NMR spectrum of complex C5 in CD_2Cl_2. Figure S25: ^{13}C NMR spectrum of complex **C5** in CD_2Cl_2. Figure S26: ^{31}P NMR spectrum of complex **C5** in CD_2Cl_2. Figure S27: ^{1}H NMR spectrum of complex **C6** (and homoleptic $[Cu(dppe)_2]^+$) in CD_2Cl_2. Figure S28: ^{13}C NMR spectrum of complex **C6** (and homoleptic $[Cu(dppe)_2]^+$) in CD_2Cl_2. Figure S29: ^{31}P NMR spectrum of complex **C6** (and homoleptic $[Cu(dppe)_2]^+$) in CD_2Cl_2. Figure S30: ^{11}B NMR spectrum in CD_2Cl_2 which is identical for the complexes **C1**–**C6**. Figure S31: ^{19}F NMR spectrum in CD_2Cl_2 which is identical for the complexes **C1**–**C6**. Figure S32: ESI-MS spectrum for complex **C1**. Figure S33: ESI-MS spectrum for complex **C2**. Figure S34: ESI-MS spectrum for complex **C3**. Figure S35: ESI-MS spectrum for complex **C4**. Figure S36: ESI-MS spectrum for complex **C5**. Figure S37: ESI-MS spectrum for complex **C6**. Figure S38: FT-IR spectrum for complex **C1**. Figure S39: FT-IR spectrum for complex **C2**. Figure S40: FT-IR spectrum for complex **C3**. Figure S41: FT-IR spectrum for complex **C4**. Figure S42: FT-IR spectrum for complex **C5**. Figure S43: FT-IR spectrum for complex **C6.**

Author Contributions: S.S.M.B.: conceptualization, methodology, complex syntheses, fluorescence emission spectrum measurement, data curation, visualisation, writing—original draft preparation, writing—review and editing; J.V.C.: formal analysis, ligand synthesis and characterisation; C.F. and A.-L.L.: UV-Vis absorption measurements and formal analysis, writing—review and editing; C.S.: supervision, project administration, resources, visualisation, writing—review and editing, writing—final draft. All authors have read and agreed to the published version of the manuscript.

Funding: This research received no external funding.

Institutional Review Board Statement: Not applicable.

Informed Consent Statement: Not applicable.

Data Availability Statement: The original contributions presented in this study are included in the article or the Supplementary Materials. Further inquiries can be directed to the corresponding authors.

Conflicts of Interest: The authors declare no conflicts of interest.

Abbreviations

The following abbreviations and units are used in this manuscript:

ATRA	Atom-transfer radical addition
D	Debye
DCM	Dichloromethane
DMF	Dimethylformamide
DMSO	Dimethylsulfoxide
eV	Electron Volt

FT-IR	Fourier Transform Infrared Spectroscopy
HER	Hydrogen Evolution Reaction
MeOH	Methanol
MLCT	Metal-to-ligand charge transfer
NMR	Nuclear Magnetic Resonance Spectroscopy
nm	Nanometre
UV-Vis	Ultraviolet–Visible Spectroscopy

References

1. Akita, M.; Ceroni, P.; Stephenson, C.R.J.; Masson, G. Progress in photocatalysis for organic chemistry. *J. Org. Chem.* **2023**, *88*, 6281–6283. [CrossRef] [PubMed]
2. Beatty, J.W.; Stephenson, C.R.J. Amine functionalization via oxidative photoredox catalysis: Methodology development and complex molecule synthesis. *Acc. Chem. Res.* **2015**, *48*, 1474–1484. [CrossRef] [PubMed]
3. Prier, C.K.; Rankic, D.A.; MacMillan, D.W.C. Visible light photoredox catalysis with transition metal complexes: Applications in organic synthesis. *Chem. Rev.* **2013**, *113*, 5322–5363. [CrossRef]
4. Bawden, J.C.; Francis, P.S.; DiLuzio, S.; Hayne, D.J.; Doeven, E.H.; Truong, J.; Alexander, R.; Henderson, L.C.; Gómez, D.E.; Massi, M.; et al. Reinterpreting the fate of iridium(iii) photocatalysts–screening a combinatorial library to explore light-driven side-reactions. *J. Am. Chem. Soc.* **2022**, *144*, 11189–11202. [CrossRef]
5. Hopkinson, M.N.; Tlahuext-Aca, A.; Glorius, F. Merging visible light photoredox and gold catalysis. *Acc. Chem. Res.* **2016**, *49*, 2261–2272. [CrossRef] [PubMed]
6. Teegardin, K.; Day, J.I.; Chan, J.; Weaver, J. Advances in photocatalysis: A microreview of visible light mediated ruthenium and iridium catalyzed organic transformations. *Org. Process Res. Dev.* **2016**, *20*, 1156–1163. [CrossRef]
7. Hossain, A.; Bhattacharyya, A.; Reiser, O. Copper's rapid ascent in visible-light photoredox catalysis. *Science* **2019**, *364*, eaav9713. [CrossRef]
8. Sandoval-Pauker, C.; Molina-Aguirre, G.; Pinter, B. Status report on copper (i) complexes in photoredox catalysis; photophysical and electrochemical properties and future prospects. *Polyhedron* **2021**, *199*, 115105. [CrossRef]
9. McMillin, D.R.; McNett, K.M. Photoprocesses of copper complexes that bind to DNA. *Chem. Rev.* **1998**, *98*, 1201–1220. [CrossRef]
10. McMillin, D.R.; Buckner, M.T.; Ahn, B.T. A light-induced redox reaction of bis(2,9-dimethyl-1,10-phenanthroline)copper(i). *Inorg. Chem.* **1977**, *16*, 943–945. [CrossRef]
11. Dietrich-Buchecker, C.O.; Marnot, P.A.; Sauvage, J.-P.; Kirchhoff, J.R.; McMillin, D.R. Bis(2,9-diphenyl-1,10-phenanthroline)copper(i): A copper complex with a long-lived charge-transfer excited state. *J. Chem. Soc. Chem. Commun.* **1983**, 513–515. [CrossRef]
12. Kuang, S.-M.; Cuttell, D.G.; McMillin, D.R.; Fanwick, P.E.; Walton, R.A. Synthesis and structural characterization of cu(i) and ni(ii) complexes that contain the bis[2-(diphenylphosphino)phenyl]ether ligand. Novel emission properties for the cu(i) species. *Inorg. Chem.* **2002**, *41*, 3313–3322. [CrossRef] [PubMed]
13. Miller, M.T.; Gantzel, P.K.; Karpishin, T.B. Effects of sterics and electronic delocalization on the photophysical, structural, and electrochemical properties of 2,9-disubstituted 1,10-phenanthroline copper(i) complexes. *Inorg. Chem.* **1999**, *38*, 3414–3422. [CrossRef] [PubMed]
14. Mara, M.W.; Fransted, K.A.; Chen, L.X. Interplays of excited state structures and dynamics in copper(i) diimine complexes: Implications and perspectives. *Coord. Chem. Rev.* **2015**, *282–283*, 2–18. [CrossRef]
15. Zhang, Y.; Schulz, M.; Wächtler, M.; Karnahl, M.; Dietzek, B. Heteroleptic diimine–diphosphine cu(i) complexes as an alternative towards noble-metal based photosensitizers: Design strategies, photophysical properties and perspective applications. *Coord. Chem. Rev.* **2018**, *356*, 127–146. [CrossRef]
16. Zhao, Y.-H.; Li, H.-Y.; Young, D.J.; Cao, X.; Zhu, D.-L.; Ren, Z.-G.; Li, H.-X. Heteroleptic copper(i) complexes [cu(dmp)(n^p)]bf4 for photoinduced atom-transfer radical addition reactions. *Dalton Trans.* **2023**, *52*, 8142–8154. [CrossRef]
17. Giereth, R.; Reim, I.; Frey, W.; Junge, H.; Tschierlei, S.; Karnahl, M. Remarkably long-lived excited states of copper photosensitizers containing an extended π-system based on an anthracene moiety. *Sustain. Energy Fuels* **2019**, *3*, 692–700. [CrossRef]
18. Sosoe, J.; Cruché, C.; Morin, É.; Collins, S.K. Evaluating heteroleptic copper(i)-based complexes bearing π-extended diimines in different photocatalytic processes. *Can. J. Chem.* **2020**, *98*, 461–465. [CrossRef]
19. Pfleiderer, W. Pteridines. Properties, reactivities, and biological significance. *J. Heterocycl. Chem.* **1992**, *29*, 583–605. [CrossRef]
20. Pfleiderer, W.; Zondler, H.; Mengel, R. Pteridine, xxxix. Synthese und struktur von pterin-carbonsäure-(6) und -(7). *Liebigs Ann. Chem.* **1970**, *741*, 64–78. [CrossRef]

21. Serrano, M.P.; Lorente, C.; Morán Vieyra, F.E.; Borsarelli, C.D.; Thomas, A.H. Photosensitizing properties of biopterin and its photoproducts using 2′-deoxyguanosine 5′-monophosphate as an oxidizable target. *Phys. Chem. Chem. Phys.* **2012**, *14*, 11657–11665. [CrossRef] [PubMed]
22. Nichol, C.A.; Smith, G.K.; Duch, D.S. Biosynthesis and metabolism of tetrahydrobiopterin and molybdopterin. *Annu. Rev. Biochem.* **1985**, *54*, 729–764. [CrossRef] [PubMed]
23. Lorente, C.; Thomas, A.H. Photophysics and photochemistry of pterins in aqueous solution. *Acc. Chem. Res.* **2006**, *39*, 395–402. [CrossRef] [PubMed]
24. Godoy-Ortega, G.; Rodríguez-Muñiz, G.M.; Lhiaubet-Vallet, V.; Lorente, C.; Thomas, A.H. Pterin–thymidine adducts: From their photochemical synthesis to their photosensitizing properties. *J. Phys. Chem. B* **2025**, *129*, 3334–3344. [CrossRef]
25. Choi, S.-W.; Mason, J.B. Folate and carcinogenesis: An integrated scheme. *J. Nutr.* **2000**, *130*, 129–132. [CrossRef]
26. Colston, K.J.; Basu, P. Synthesis, redox and spectroscopic properties of pterin of molybdenum cofactors. *Molecules* **2022**, *27*, 3324. [CrossRef]
27. Andrade, P.; Carneiro, M. Pterin-based pigmentation in animals. *Biol. Lett.* **2021**, *17*, 20210221. [CrossRef]
28. Kosuge, T.; Tsuji, K.; Hirai, K.; Yamaguchi, K.; Okamoto, T.; Iitaka, Y. Isolation and structure determination of a new marine toxin, neosurugatoxin, from the japanese ivory shell, babylonia japonica. *Tetrahedron Lett.* **1981**, *22*, 3417–3420. [CrossRef]
29. Black, K.J.; Huang, H.; High, S.; Starks, L.; Olson, M.; McGuire, M.E. Ruthenium(ii) complexes of a fused phenanthroline-pteridinedione ligand. *Inorg. Chem.* **1993**, *32*, 5591–5596. [CrossRef]
30. Gao, F.; Chao, H.; Zhou, F.; Yuan, Y.-X.; Peng, B.; Ji, L.-N. DNA interactions of a functionalized ruthenium(ii) mixed-polypyridyl complex [ru(bpy)2ppd]2+. *J. Inorg. Biochem.* **2006**, *100*, 1487–1494. [CrossRef]
31. Gao, F.; Chao, H.; Zhou, F.; Xu, L.-C.; Zheng, K.-C.; Ji, L.-N. Synthesis, characterization, and DNA-binding properties of the chiral ruthenium(ii) complexes δ- and λ-[ru(bpy)2(dmppd)]2+ (dmppd = 10,12-dimethylpteridino[6,7-f] [1,10]phenanthroline-11,13(10h,12h)-dione; bpy = 2,2′-bipyridine). *Helv. Chim. Acta* **2007**, *90*, 36–51. [CrossRef]
32. Dalton, S.R.; Glazier, S.; Leung, B.; Win, S.; Megatulski, C.; Burgmayer, S.J.N. DNA binding by ru(ii)–bis(bipyridine)–pteridinyl complexes. *J. Biol. Inorg. Chem.* **2008**, *13*, 1133–1148. [CrossRef] [PubMed]
33. Ragone, F.; Yañuk, J.G.; Cabrerizo, F.M.; Prieto, E.; Wolcan, E.; Ruiz, G.T. DNA structural changes (photo)induced by tricarbonyl (pterin)rhenium(i) complex. *J. Inorg. Biochem.* **2024**, *252*, 112471. [CrossRef]
34. Forero Cortés, P.A.; Marx, M.; Trose, M.; Beller, M. Heteroleptic copper complexes with nitrogen and phosphorus ligands in photocatalysis: Overview and perspectives. *Chem Catalysis* **2021**, *1*, 298–338. [CrossRef]
35. Henriquez, M.A.; Engl, S.; Jaque, P.; Gonzalez, I.A.; Natali, M.; Reiser, O.; Cabrera, A.R. Phosphine evaluation on a new series of heteroleptic copper(i) photocatalysts with dpa ligand [cu(dpa)(p,p)]bf4. *Eur. J. Inorg. Chem.* **2021**, *2021*, 4020–4029. [CrossRef]
36. Xiao, P.; Dumur, F.; Zhang, J.; Fouassier, J.P.; Gigmes, D.; Lalevée, J. Copper complexes in radical photoinitiating systems: Applications to free radical and cationic polymerization upon visible leds. *Macromolecules* **2014**, *47*, 3837–3844. [CrossRef]
37. Nonogawa, M.; Arai, T.; Endo, N.; Pack, S.P.; Kodaki, T.; Makino, K. Hydrogen bond removal of pterin derivative whose structure is similar to nucleic acid bases. *Nucleic Acids Symp. Ser.* **2005**, *49*, 311–312. [CrossRef]
38. Seo, T.; Toyoshima, N.; Kubota, K.; Ito, H. Tackling solubility issues in organic synthesis: Solid-state cross-coupling of insoluble aryl halides. *J. Am. Chem. Soc.* **2021**, *143*, 6165–6175. [CrossRef]
39. DeGroot, H.P.; Hanusa, T.P. Solvate-assisted grinding: Metal solvates as solvent sources in mechanochemically driven organometallic reactions. *Organometallics* **2021**, *40*, 3516–3525. [CrossRef]
40. Gomollón-Bel, F. Ten chemical innovations that will change our world: Iupac identifies emerging technologies in chemistry with potential to make our planet more sustainable. *Chem. Int.* **2019**, *41*, 12–17. [CrossRef]
41. Ferguson, M.; Giri, N.; Huang, X.; Apperley, D.; James, S.L. One-pot two-step mechanochemical synthesis: Ligand and complex preparation without isolating intermediates. *Green Chem.* **2014**, *16*, 1374–1382. [CrossRef]
42. Cuccu, F.; De Luca, L.; Delogu, F.; Colacino, E.; Solin, N.; Mocci, R.; Porcheddu, A. Mechanochemistry: New tools to navigate the uncharted territory of "impossible" reactions. *ChemSusChem* **2022**, *15*, e202200362. [CrossRef]
43. Al Jomeh, G.A.S.; McGown, A.; Richards, E.; Tizzard, G.J.; Coles, S.J.; González-Méndez, R.; Dadswell, C.; Spencer, J.; Kostakis, G.E. Mechanochemical cu(ii) complexes and propargylamine synthetic adventures. *RSC Sustain.* **2024**, *2*, 528–535. [CrossRef]
44. Kazimi, S.G.T.; Iqbal, M.S.; Mulligan, C.C.; Baseer, M.; Rehman, A.U.; Farooqi, F.; Person, J.R. Mechanochemical synthesis of six cu(ii) complexes with selected thiols, their physicochemical characterization and interaction with DNA. *J. Mol. Struct.* **2022**, *1265*, 133436. [CrossRef]
45. Remy-Speckmann, I.; Zimmermann, B.M.; Gorai, M.; Lerch, M.; Teichert, J.F. Mechanochemical solid state synthesis of copper(i)/nhc complexes with k3po4. *Beilstein J. Org. Chem.* **2023**, *19*, 440–447. [CrossRef]
46. Liao, Q.; Su, K.; Cai, H.; Zhao, T.; Liu, F. Mechanochemical synthesis of carbene copper complexes for co2 hydrogenation to formate. *J. CO2 Util.* **2022**, *59*, 101963. [CrossRef]
47. Jaros, S.W.; Sokolnicki, J.; Siczek, M.; Smoleński, P. Strategy for an effective eco-optimized design of heteroleptic cu(i) coordination polymers exhibiting thermally activated delayed fluorescence. *Inorg. Chem.* **2023**, *62*, 19898–19907. [CrossRef]

48. Kobayashi, A.; Hasegawa, T.; Yoshida, M.; Kato, M. Environmentally friendly mechanochemical syntheses and conversions of highly luminescent cu(i) dinuclear complexes. *Inorg. Chem.* **2016**, *55*, 1978–1985. [CrossRef]
49. Garra, P.; Dumur, F.; Al Mousawi, A.; Graff, B.; Gigmes, D.; Morlet-Savary, F.; Dietlin, C.; Fouassier, J.P.; Lalevée, J. Mechanosynthesized copper(i) complex based initiating systems for redox polymerization: Towards upgraded oxidizing and reducing agents. *Polym. Chem.* **2017**, *8*, 5884–5896. [CrossRef]
50. Zeng, C.; Wang, N.; Peng, T.; Wang, S. Copper(i) complexes bearing 1,2-phenyl-bridged p∧n, p∧n∧p, and n∧p∧n chelate ligands: Structures and phosphorescence. *Inorg. Chem.* **2017**, *56*, 1616–1625. [CrossRef]
51. Garra, P.; Dumur, F.; Morlet-Savary, F.; Dietlin, C.; Gigmes, D.; Fouassier, J.P.; Lalevée, J. Mechanosynthesis of a copper complex for redox initiating systems with a unique near infrared light activation. *J. Polym. Sci. Polym. Chem.* **2017**, *55*, 3646–3655. [CrossRef]
52. Garra, P.; Dumur, F.; Mokbel, H.; Monnier, V.; Morlet-Savary, F.; Dietlin, C.; Gigmes, D.; Fouassier, J.-P.; Lalevée, J. New synthetic route to an highly efficient photoredox catalyst by mechanosynthesis. *ACS Omega* **2018**, *3*, 10938–10944. [CrossRef]
53. Correia, J.V.; Bandaru, S.S.M.; Schulzke, C. Pushing at the boundaries of pterin chemistry. *Molecules* **2024**, *29*, 4587. [CrossRef]
54. Kaeser, A.; Mohankumar, M.; Mohanraj, J.; Monti, F.; Holler, M.; Cid, J.-J.; Moudam, O.; Nierengarten, I.; Karmazin-Brelot, L.; Duhayon, C.; et al. Heteroleptic copper(i) complexes prepared from phenanthroline and bis-phosphine ligands. *Inorg. Chem.* **2013**, *52*, 12140–12151. [CrossRef]
55. Pianet, I.; Vincent, J.-M. Isomerization dynamics in homo- and heterochiral atropoisomer copper(i) diimine complexes: A 2d exsy nmr study. *Inorg. Chem.* **2004**, *43*, 2947–2953. [CrossRef]
56. Comba, P.; Katsichtis, C.; Nuber, B.; Pritzkow, H. Solid-state and solution structural properties of copper(i) compounds with bidentate phosphane ligands. *Eur. J. Inorg. Chem.* **1999**, *1999*, 777–783. [CrossRef]
57. Listorti, A.; Accorsi, G.; Rio, Y.; Armaroli, N.; Moudam, O.; Gégout, A.; Delavaux-Nicot, B.; Holler, M.; Nierengarten, J.-F. Heteroleptic copper(i) complexes coupled with methano[60]fullerene: Synthesis, electrochemistry, and photophysics. *Inorg. Chem.* **2008**, *47*, 6254–6261. [CrossRef]
58. Moudam, O.; Kaeser, A.; Delavaux-Nicot, B.; Duhayon, C.; Holler, M.; Accorsi, G.; Armaroli, N.; Séguy, I.; Navarro, J.; Destruel, P.; et al. Electrophosphorescent homo- and heteroleptic copper(i) complexes prepared from various bis-phosphine ligands. *Chem. Commun.* **2007**, 3077–3079. [CrossRef]
59. Sandroni, M.; Kayanuma, M.; Rebarz, M.; Akdas-Kilig, H.; Pellegrin, Y.; Blart, E.; Le Bozec, H.; Daniel, C.; Odobel, F. Heteroleptic diimine copper(i) complexes with large extinction coefficients: Synthesis, quantum chemistry calculations and physico-chemical properties. *Dalton Trans.* **2013**, *42*, 14628–14638. [CrossRef]
60. Leoni, E.; Mohanraj, J.; Holler, M.; Mohankumar, M.; Nierengarten, I.; Monti, F.; Sournia-Saquet, A.; Delavaux-Nicot, B.; Nierengarten, J.-F.i.; Armaroli, N. Heteroleptic copper(i) complexes prepared from phenanthroline and bis-phosphine ligands: Rationalization of the photophysical and electrochemical properties. *Inorg. Chem.* **2018**, *57*, 15537–15549. [CrossRef]
61. Zhang, K.; Zhang, D. Synthesis and study on a series of phosphorescent cu(i) complexes having sterically blocking ligands. *Spectrochim. Acta Part A-Mol. Biomol. Spectrosc.* **2014**, *124*, 341–348. [CrossRef]
62. Alconchel, A.; Crespo, O.; Gimeno, M.C. Thermally activated delayed fluorescence in neutral and cationic copper(i) complexes with the 2-(4-thiazolyl)benzimidazole ligand. *Inorg. Chem.* **2023**, *62*, 10431–10439. [CrossRef]
63. Siddique, Z.A.; Yamamoto, Y.; Ohno, T.; Nozaki, K. Structure-dependent photophysical properties of singlet and triplet metal-to-ligand charge transfer states in copper(i) bis(diimine) compounds. *Inorg. Chem.* **2003**, *42*, 6366–6378. [CrossRef] [PubMed]
64. Harris, R.K.; Becker, E.D.; Cabral De Menezes, S.M.; Goodfellow, R.; Granger, P. Nmr nomenclature: Nuclear spin properties and conventions for chemical shifts (iupac recommendations 2001). *Concepts Magn. Reson.* **2002**, *14*, 326–346. [CrossRef]
65. Bandaru, S.S.M.; Bhilare, S.; Chrysochos, N.; Gayakhe, V.; Trentin, I.; Schulzke, C.; Kapdi, A.R. Pd/ptabs: Catalyst for room temperature amination of heteroarenes. *Org. Lett.* **2018**, *20*, 473–476. [CrossRef] [PubMed]
66. Sokolovs, I.; Suna, E. Para-selective cu-catalyzed c–h aryloxylation of electron-rich arenes and heteroarenes. *J. Org. Chem.* **2016**, *81*, 371–379. [CrossRef]
67. da Silva Miranda, F.; Signori, A.M.; Vicente, J.; de Souza, B.; Priebe, J.P.; Szpoganicz, B.; Gonçalves, N.S.; Neves, A. Synthesis of substituted dipyrido[3,2-a:2′,3′-c]phenazines and a new heterocyclic dipyrido[3,2-f:2′,3′-h]quinoxalino[2,3-b]quinoxaline. *Tetrahedron* **2008**, *64*, 5410–5415. [CrossRef]

Disclaimer/Publisher's Note: The statements, opinions and data contained in all publications are solely those of the individual author(s) and contributor(s) and not of MDPI and/or the editor(s). MDPI and/or the editor(s) disclaim responsibility for any injury to people or property resulting from any ideas, methods, instructions or products referred to in the content.